Materials Letters 124 (2014) 126–128

Contents lists available at ScienceDirect

Materials Letters

journal homepage: www.elsevier.com/locate/matlet

Unique electromagnetic properties of the zinc ferrite nanofiber

Xiaogu Huang [a,*], Jing Zhang [b], Shaorong Xiao [a], Tianyi Sang [c], Guosheng Chen [a]

[a] School of Physics and Optoelectronic Engineering, Nanjing University of Information Science & Technology, Nanjing 210044, China
[b] Nanjing Center, China Geological Survey, Nanjing 210016, China
[c] School of Electronic and Optical Engineering, Nanjing University of Science and Technology, Nanjing 210094, China

ARTICLE INFO

Article history:
Received 28 January 2014
Accepted 8 March 2014
Available online 17 March 2014

Keywords:
Ceramics
Functional
Ferrite
Nanofiber
Electromagnetic properties
Microwave absorption

ABSTRACT

The $ZnFe_2O_4$ ferrite nanoparticle and nanofiber were synthesized by electrospinning method. The phase composition, morphology, magnetic and electromagnetic properties were analyzed. The results showed that both the samples exhibited a pure phase of spinel type ferrite. The $ZnFe_2O_4$ ferrite nanoparticle was aggregated, while the $ZnFe_2O_4$ ferrite nanofiber performed the homogeneous nano-fibrous shape as well as single-particle-chain structure. The magnetic analysis indicated that the $ZnFe_2O_4$ ferrite nanofiber showed ferromagnetic behaviour. Moreover, the dielectric loss and magnetic loss properties of $ZnFe_2O_4$ ferrite nanofiber were both enhanced due to its better dipole polarization, interfacial polarization and shape anisotropy.

1. Introduction

Ferromagnetic resonance and dielectric relaxation are well-known mechanisms normally responsible for microwave absorption [1,2]. However, Zinc ferrite, $ZnFe_2O_4$, is not among the high efficient microwave absorbing material candidates because of its paramagnetic property and poor dielectric loss ability. To improve the electromagnetic properties of $ZnFe_2O_4$ ferrite in the GHz frequency, a common approach was to change the ions distribution between the A-site and B-site in the spinel structure via doping magnetic ions. For example, the ferromagnetic properties were discovered in the Ni^{2+}-doped, Co^{2+}-doped and Mn^{2+}-doped $ZnFe_2O_4$ ferrite [3–5]. However, the dielectric loss cannot be evidently enhanced, meanwhile the doping process was easy to introduce impurity and damage the spinel structure.

Here, one-dimension nanostructure was adopted to directly improve the electromagnetic properties of $ZnFe_2O_4$ ferrite. By comparing with the morphology, magnetic and electromagnetic properties between the zinc ferrite nanoparticle (NP) and nanofiber (NF), we demonstrate that the single-particle-chain structure has more interface than single particle. The dielectric loss and magnetic loss properties of the spinel ferrite nanofiber were both enhanced due to its better dipole polarization, interfacial polarization and shape anisotropic. This study may also expand the applications of $ZnFe_2O_4$ into new areas in gas sensing [6], magnetic behavior [7], electrical characteristics [8] and semiconductor photocatalysis [9].

2. Experimental

The $ZnFe_2O_4$ ferrite nanoparticle and nanofiber were synthesized by the electrospinning method. First, the metal salt solution was prepared by dissolving the 0.01 mol $C_4H_6O_4Zn \cdot 2H_2O$ and 0.02 mol $FeCl_3 \cdot 6H_2O$ into the 20 ml *N*,*N*-dimethylformamide (DMF). Second, different amount polyvinylpyrrolidone (PVP, K-30) was added in 36 ml anhydrous alcohol to prepare the PVP solution. To obtain the $ZnFe_2O_4$ ferrite nanoparticle, the amount of PVP was 5.0 g. While, the 9.0 g PVP was using to prepare the $ZnFe_2O_4$ ferrite nanofiber. Then, the spinning solution was obtained after the as-prepared metal salt solution and PVP solution were mixed and stirred for 5 h. Third, the spinning solution was electrospun to prepare the precursor. The applied positive voltage was 12 kV, the feed rate was 3 ml/h, and the distance from needle tip to collector was 13 cm. Finally, the precursor were dried at 80 °C for 7 h and then calcined at 700 °C for 2 h with a heating rate of 2 °C/min.

The X-ray diffraction analysis was carried out using an X-ray powder diffractometer (XRD, Rigaka, D/MAX2500). The morphology was observed using a transmission electron microscope (TEM, FEI Tecnai G2 F30) and a field emission scanning electron microscopy (FE-SEM, HITACHI S-4800). Magnetic properties were tested by vibrating sample magnetometer (VSM, Lakeshore 7307–9309). The electromagnetic parameters (ε', ε'', μ', μ'') were measured by a Network analyzer (Agilent PNA 8363B) in the frequency range of

* Corresponding author. Tel./fax: +86 25 83587246.
E-mail address: nthxg@126.com (X. Huang).

http://dx.doi.org/10.1016/j.matlet.2014.03.049
0167-577X/

2–18 GHz. The samples were prepared by uniformly mixing 85 wt% of paraffin and 15 wt% of ferrite nanofiber, and then pressed in a cylindrical mold with a size of 3 mm (inside) × 7 mm (outside) × 2 mm (height). The measured values of reflected and transmitted scattering parameters (S_{11}, S_{21}) were used to determine the electromagnetic parameters [10].

3. Results and discussion

The phase composition is identified by the XRD. From Fig. 1, there is no impurity phase presented in the spectra, and all the diffraction peaks can be indexed to the zinc ferrite (JCPDS No. 65-3111). It is indicated that both the as-synthesized $ZnFe_2O_4$ ferrite nanoparticle and nanofiber have a pure phase of spinel ferrite.

Morphologies of samples were measured by FE-SEM and TEM. As shown in Fig. 2(a), the as-prepared $ZnFe_2O_4$ ferrite nanoparticle was aggregated, and the nanoparticle size was nearly 80 nm. For the $ZnFe_2O_4$ ferrite nanofiber, it can be seen from Fig. 2(b) that the sample exhibited the typical and homogeneous nano-fibrous shape as well as high length–diameter ratio. The diameter of the nanofiber was about 80 nm. The TEM analysis indicated that the as-prepared $ZnFe_2O_4$ ferrite nanofiber possessed single-particle-chain structure, and there were many interfaces among the single particles (Fig. 2(c)). From Fig. 2(d), the HRTEM image revealed that the spinel ferrite phase was highly crystallized. The spacing values of 0.25 nm depicted the lattice-resolved (311) crystalline plane.

The magnetic property of the $ZnFe_2O_4$ ferrite nanofibers was determined by VSM at room temperature, and its hysteresis loop was presented in Fig. 3. It is striking to note that the $ZnFe_2O_4$

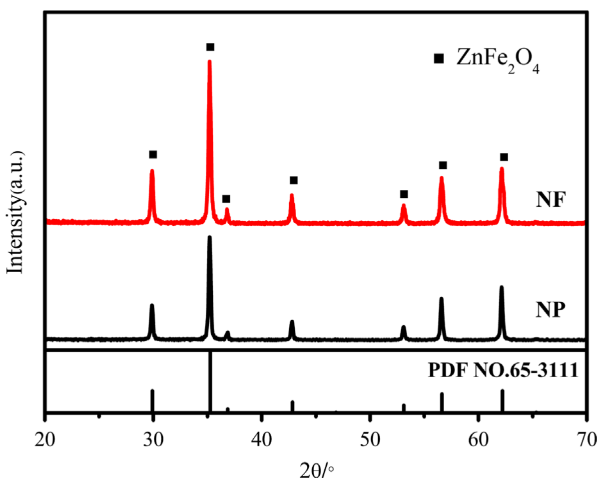

Fig. 1. XRD spectra of the $ZnFe_2O_4$ ferrite nanoparticle and nanofiber.

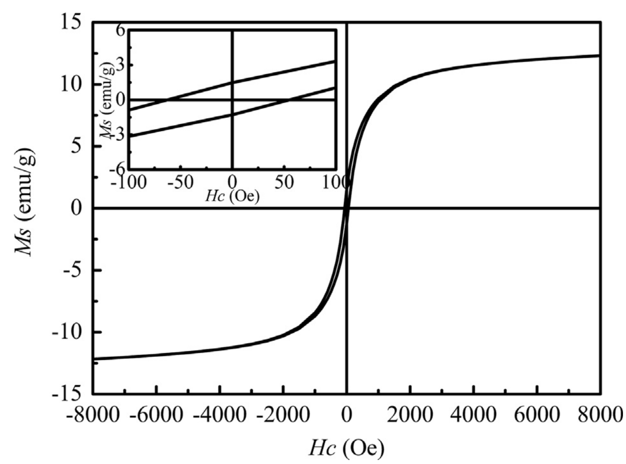

Fig. 3. Magnetic hysteresis loop of the $ZnFe_2O_4$ ferrite nanofiber at room temperature.

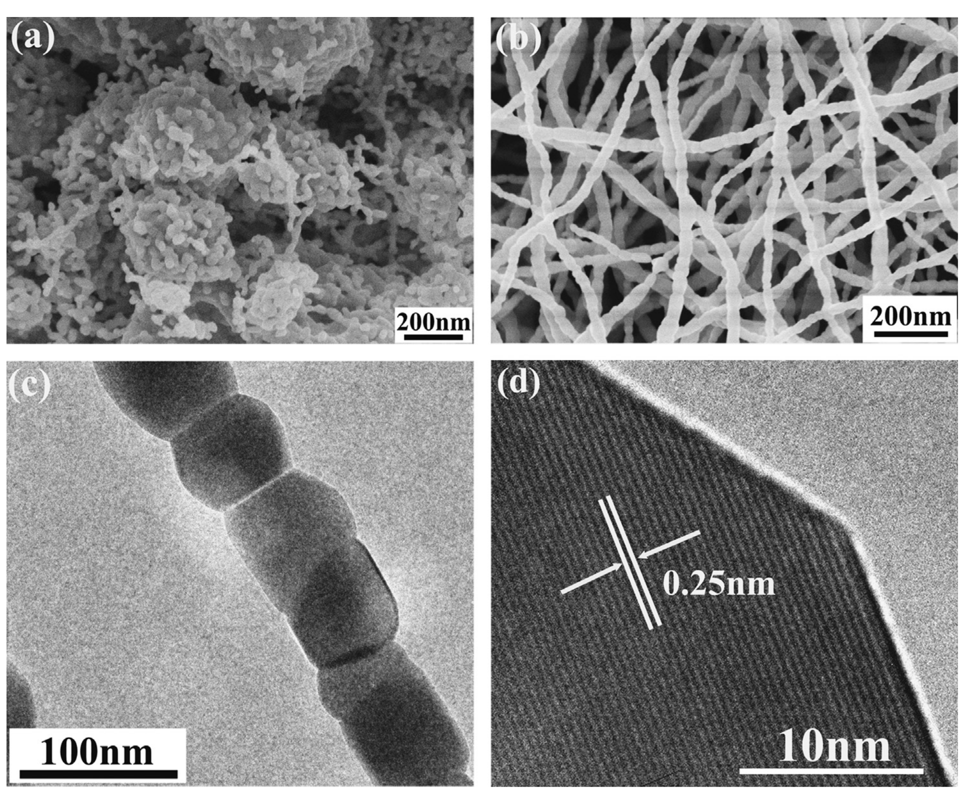

Fig. 2. (a) FE-SEM image of $ZnFe_2O_4$ ferrite nanoparticle, (b) FE-SEM image, (c) TEM image, (d) HRTEM image of $ZnFe_2O_4$ ferrite nanopfiber.

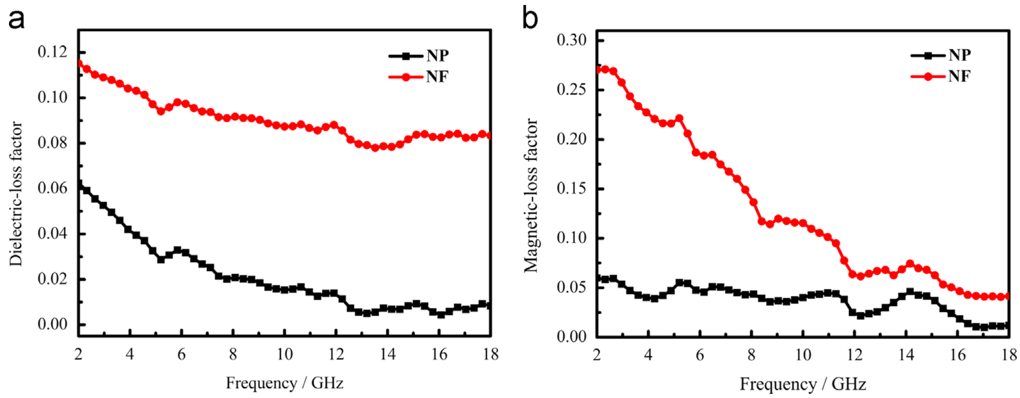

Fig. 4. (a) Dielectric loss factor and (b) magnetic loss factor of $ZnFe_2O_4$ ferrite nanoparticle and nanofiber.

ferrite nanofibers behave as a significant hysteresis loop, indicating the ferromagnetic property. As well known, the traditional $ZnFe_2O_4$ ferrite particle usually shows paramagnetic property. However, previous studies have confirmed that the nanocrystalline $ZnFe_2O_4$ could exhibit ferromagnetic property due to the effects of small grain size on the cation distribution and magnetic properties [11,12]. Here, our research also in conformity with these studies. The saturation magnetization (M_s) was nearly 12.4 emu/g and the coercivity (H_c) was about 48.79 Oe.

To investigate the electromagnetic loss properties, the dielectric loss property and magnetic loss property were usually characterized by dielectric loss factor ($\tan\delta_\varepsilon = \varepsilon''/\varepsilon'$) and magnetic loss factor ($\tan\delta_u = \mu''/\mu'$), respectively [13,14]. The ε' and ε'' are the real part and the imaginary part of the complex permittivity, and the μ' and μ'' are the real part and the imaginary part of the complex permeability, respectively. The complex permittivity and the complex permeability of the $ZnFe_2O_4$ ferrite nanoparticle and nanofiber were investigated in the frequency range of 2–18 GHz, and the results were shown in Fig. S1. Then, the dielectric loss factor and magnetic loss factor were calculated. From Fig. 4(a), the dielectric loss factor of $ZnFe_2O_4$ ferrite nanoparticle was nearly 0.01–0.06. However, the dielectric loss factor of $ZnFe_2O_4$ ferrite nanofiber was increased to 0.09–0.12. This value was also larger than that of the $Ni_{0.6}Zn_{0.4}Fe_2O_4$ octahedral nanoparticle (0.00–0.06) and NiZn–ferrite nanocrystallines (0.01–0.09) [15,16]. It can be ascribed to the following three reasons. First, the migration between the Fe^{3+} and Zn^{2+} ions can introduce the intrinsic electric dipole, causing the dipole polarization in the $ZnFe_2O_4$ ferrite nanofiber. Second, the orientational polarization can be improved due to the large shape anisotropic [17]. Third, the single-particle-chain structure has more interface than single particle, and the interfacial polarization was beneficial for the attenuation of microwave power.

Moreover, it can be found from Fig. 2(b) that the magnetic loss property of $ZnFe_2O_4$ ferrite nanofiber was also stronger than which of $ZnFe_2O_4$ ferrite nanoparticle. In generally, natural resonance of ferrite was the main mechanism for the magnetic loss. According to the Larmor equation, natural-resonance frequency (f_r) can be expressed as: $f_r = (\gamma H_a)/2\pi$, where γ is the gyromagnetic ratio and H_a is the effective anisotropic field [18]. The effective anisotropic field of the $ZnFe_2O_4$ ferrite nanofiber was enhanced due to its high length–diameter ratio and large shape anisotropic. As a result, the $ZnFe_2O_4$ ferrite nanofiber performed stronger magnetic loss property.

4. Conclusion

The $ZnFe_2O_4$ nanoparticle and nanofiber with a pure phase of spinel type ferrite were successfully synthesized by the electrospinning method. The $ZnFe_2O_4$ ferrite nanofiber exhibited the unique single-particle-chain structure and behaved as the ferromagnetic property. The dielectric loss and magnetic loss properties of $ZnFe_2O_4$ ferrite nanofiber were both stronger than that of $ZnFe_2O_4$ ferrite nanoparticle due to its better dipole polarization, interfacial polarization and shape anisotropic. This work gives a novel insight to improve the electromagnetic properties of ferrite, and the as-prepared $ZnFe_2O_4$ ferrite nanofiber can be potentially used as a lightweight microwave absorbing material.

Acknowledgments

We are deeply grateful to Jianqing Jiang at the Nanjing University of Information Science & Technology for the assistance with the preparation of ferrite nanofiber. This work was financially supported by the Project Funded by the Priority Academic Program Development (PAPD) of Jiangsu Higher Education Institutions and the Scientific Research Startup Foundation of Nanjing University of Information Science & Technology (2013 × 022).

Appendix A. Supplementary Information

Supplementary data associated with this article can be found in the online version at http://dx.doi.org/10.1016/j.matlet.2014.03.049.

References

[1] Wang WJ, Gumfekar SP, Jiao QJ, Zhao BX. J Mater Chem C 2013;1:2851–9.
[2] Xia T, Zhang C, Oyler NA, Chen XB. Adv Mater 2013;25:6905–10.
[3] Sharma R, Singhal S. Physica B 2013;414:83–90.
[4] Manikandan A, Kennedy LJ, Bououdina M, Vijaya JJ. J Magn Magn Mater 2014;349:249–58.
[5] Dahotre SG, Singh LN. J Pure Appl Ind Phys 2013;3(3):199–204.
[6] Pileni MP. Adv Funct Mater 2001;11:323–36.
[7] Hochepied JF, Bonville P, Pileni MP. J Phys Chem B 2000;104:905–12.
[8] Yu SH, Yoshimura M. Chem Mater 2000;12:3805–10.
[9] Liu FF, Li XY, Zhao QD, Hou Y, Quan X, Chen GH. Acta Mater 2009;57:2684–90.
[10] Vanzura EJ, Baker-Jarvis JR, Grosvenor JH, Janezic MD. IEEE Trans Microw Theory Tech 1994;42:2063–70.
[11] Chinnasamy CN, Narayanasamy A, Ponpandian N, Chattopadhyay K, Guérault H, Greneche JM. J Phys Condens Mater 2000;12(35):7795–805.
[12] Wu JT, Li N, Xu J, Jiang YQ, Ye ZG, Xie ZX. Appl Phys Lett 2011;99:202505.
[13] Pan HS, Cheng XQ, Zhang CH, Gong CH, Yu LG, Zhang JW, et al. Appl Phys Lett 2013;102:012410.
[14] Liu JW, Cheng J, Che RC, Xu JJ, Liu MM, Liu ZW. J Phys Chem C 2013;117:489–95.
[15] Wang ZZ, Wu MZ, Jin SW, Li G, Ma YQ, Wang PH. J Magn Magn Mater 2013;344:101–4.
[16] Zhang M, Liu QC, Zi ZF, Dai YQ, Zhu XB, Sun YP, et al. Sci China Technol Sci 2013;56(1):13–9.
[17] Tong GX, Hua Q, Wu WH, Qin MY, Li LC, Gong PJ. Sci China Tech Sci 2011;54:484–9.
[18] Kittel C. Phys Rev 1948;73:155–61.